Article

pubs.acs.org/Biomac

Computational Design and Biosensor Applications of Small Molecule-Sensing Allosteric Ribozymes

Robert Penchovsky*

Department of Genetics, Faculty of Biology, Sofia University "St. Kliment Ohridski", 8 Dragan Tzankov Boulevard, 1164 Sofia, Bulgaria

Supporting Information

ABSTRACT: Here I describe accurate and time-efficient computational methods for designing small molecule-sensing allosteric ribozymes that serve as logic gates with NOT or YES Boolean logic functions. Theophylline-sensing ribozymes are engineered to have a high cleavage rate of 1.3 min^{-1} under physiologically relevant conditions. They are highly specific to theophylline and do not respond to caffeine, which differs in a single methyl group. These ribozymes are designed by fusing a theophylline aptamer with an extended version of the hammerhead ribozyme by modeling secondary structures. Purine-sensing ribozymes are designed by fusing the minimal version of the hammerhead ribozyme with bacterial guanine or adenine aptamers by modeling 3D interactions. I have developed high-throughput compatible arrays based on purine RNA sensors that can be used for antibacterial drug discovery. The ribozymes can be employed as molecular sensors in various applications, including exogenous control of gene expression, high-throughput screening arrays, and molecular computing.

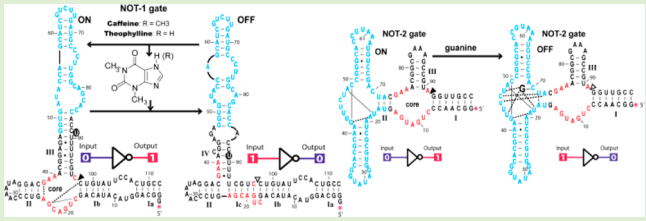

INTRODUCTION

RNA and DNA aptamers are structured nucleic acids that form selective pockets for binding target molecules, termed ligands.[1] The first known RNA aptamers were synthetic molecules obtained by in vitro selection or, equivalently, by systematic evolution of ligands by exponential enrichment (SELEX) techniques 22 years ago.[2] Over this time, many RNA aptamers were engineered to bind various ligands, including small molecules, nucleic acids, and proteins.[3] It has been proven that nucleic acids and, particularly RNA, are very suitable media for engineering diverse aptamers.[4]

The first naturally occurring aptamers were found in the untranslated region (UTR) of some bacterial mRNAs (mRNAs)[5] about 10 years ago. Their function is to control gene expression by directly binding metabolites in the framework of novel gene control elements termed riboswitches.[6] Bacterial riboswitches are believed to be promising targets for antibacterial drug discovery.[7]

Both synthetic and natural RNA aptamers can be joined with other functional RNA domains like ribozymes to serve as biosensors. Allosteric ribozymes have various applications to modern biotechnology. Such applications include detection of specific chemical compounds,[8] reporter systems for high-throughput screening (HTS) arrays,[9] exogenous control of gene expression,[10] molecular computing,[11] and others. Therefore, the methods for engineering molecular biosensors by fusing aptamer to ribozyme domains are of significant practical use.

There are different approaches for designing allosteric ribozymes. Such approaches include various in vitro selection,[12] rational design,[13] and computational methods. Here is described computational methods for designing small molecule-sensing allosteric ribozymes. The designer ribozymes are obtained by fusing synthetic or natural aptamers to the extended or minimal version of the hammerhead ribozyme.[14]

I use two different modeling steps to design small molecule-sensing ribozymes. These methods represent a logical extension of already proven and published approach for computational design of oligonucleotide-sensing ribozymes.[11,15] The first approach for designing allosteric ribozymes is based on the extended version of the hammerhead ribozyme[16] fused with the theophylline aptamer.[17] These ribozymes have high-speed kinetics of cleavage and can work in the cell. The method can generate a large number of allosteric ribozymes with predefined properties with a time scale of min on a modern personal computer.

The second method is based on modeling 3D interactions between the allosteric ribozyme and the ligand. In this case, I use the minimal version of the hammerhead ribozyme and the guanine[18] and adenine aptamers from the guanine and the adenine (the purine) riboswitches. The purine aptamers are part of riboswitches found in the untranslated region of mRNAs in 13 human pathogenic bacteria to control gene expression by directly binding guanine or adenine.[19] They are found in 5′ UTR of mRNAs in many human bacterial pathogens, including *Bacillus anthracis*, *Clostridium perfringens*, *Listeria monocytogenes*, *Staphylococcus aureus*, and many others. Therefore, finding small molecules that specifically bind purine aptamers is an important step in the antibacterial drug development process.[20]

Received: February 27, 2013
Published: March 3, 2013

dx.doi.org/10.1021/bm400299a | *Biomacromolecules* 2013, 14, 1240−1249

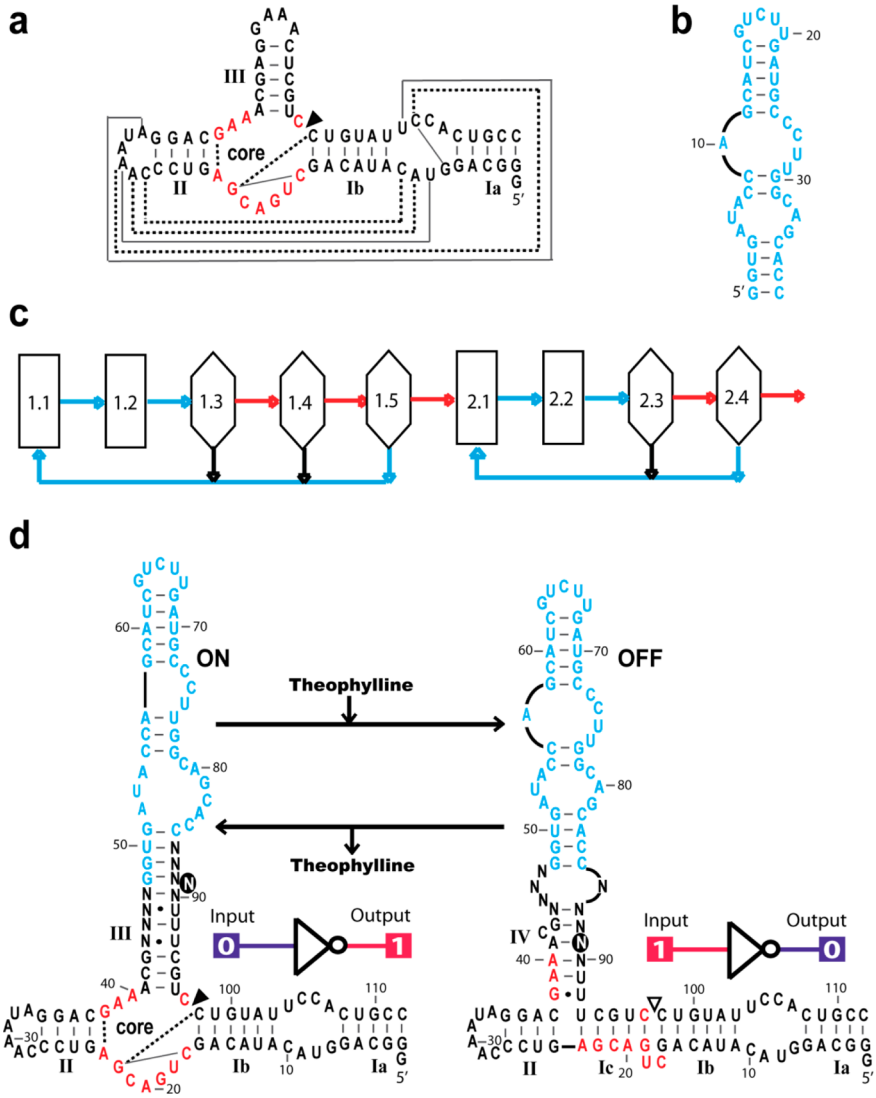

Figure 1. Computational design of theophylline-sensing high-speed hammerhead ribozymes (NOT-1). (a) Extended hammerhead ribozyme sequence used to create theophylline-responsive switches that exhibit high-speed of self-cleavage under low Mg^{2+} concentration. All canonical tertiary interactions of the ribozyme are shown by the solid lines, while the noncanonical tertiary contacts are depicted by the dashed lines. (b) The secondary structure of the theophylline-sensing aptamer is depicted in blue. (c) Algorithm employed to design the theophylline-sensing riboswitches is schematically depicted. Red arrows indicate successful fulfilling of the computational step, black arrows indicate unsuccessful fulfilling of the computational step, and blue arrows indicate unconditional pass to the next step. Hexagons define decision-making steps. Descriptions of these steps are presented in the text. (d) The ribozyme carries a theophylline-sensing aptamer embedded into stem III. All randomized nucleotides are shown as N. The switch is designed to serve as a NOT logic gate. In the absence of theophylline, all three stems are correctly formed that results in a self-cleavage (ON) state at the position indicated by the arrowhead. The aptamer sequence (in blue) reacts with theophylline and adopts its normal structure, which results in switching of the ribozyme into an inactive state by the distraction of stem III and formation of stem IV. The caffeine, which differs in a single methyl group, does not bind to the aptamer and should not affect the ribozyme self-cleavage.

MATERIALS AND METHODS

Design of RNA Switches by Modeling Secondary Structures.

The design of theophylline-sensing NOT allosteric ribozymes was performed in two steps (Figure 1c) using a random search algorithm[21] by computing RNA secondary structures based on the equilibrium partition function.[22] Our use of this approach relies on the application of thermodynamic parameters[23] using essentially the RNAfold source code from the Vienna RNA folding package.[24]

1.1 Generate a new ribozyme using the following sequence that contains the extended hammerhead motif from Schistosomes and the theophylline aptamer: 5′ggcagguacaua-agcugacgaguccaauaggacgaaacgNNNgugauaccagcaucg-cuugaugcccuuggcgcaccNNNNuucguccuguauccacugcc, where the N bases are to be randomly chosen over the alphabet of A, U, C, G (Figure 1d) and go to the next step.

1.2 Fold the sequence obtained and calculate the free energy at 37 °C of the structure using partition function and go to the next step.

1.3 Determine whether stem III (Figure 1d, ON state) of the ribozyme is formed using the probability dot matrix plot derived from the partition function. If stem III is not present, reject the sequence and go to 1.1. If stem III is present, then register the candidate sequence and go to the next step.

1.4 Determine whether stem IV (Figure 1d, OFF state) of the ribozyme is formed using the probability dot matrix plot derived from the partition function. If stem IV is not present reject the sequence and go to 1.1. If stem IV is present, then register the candidate sequence and go to the next step.

1.5 Compare the possibility of forming stems III and IV (Figure 1d, OFF state) by using the probability dot matrix plot derived

dx.doi.org/10.1021/bm400299a | *Biomacromolecules* 2013, 14, 1240−1249

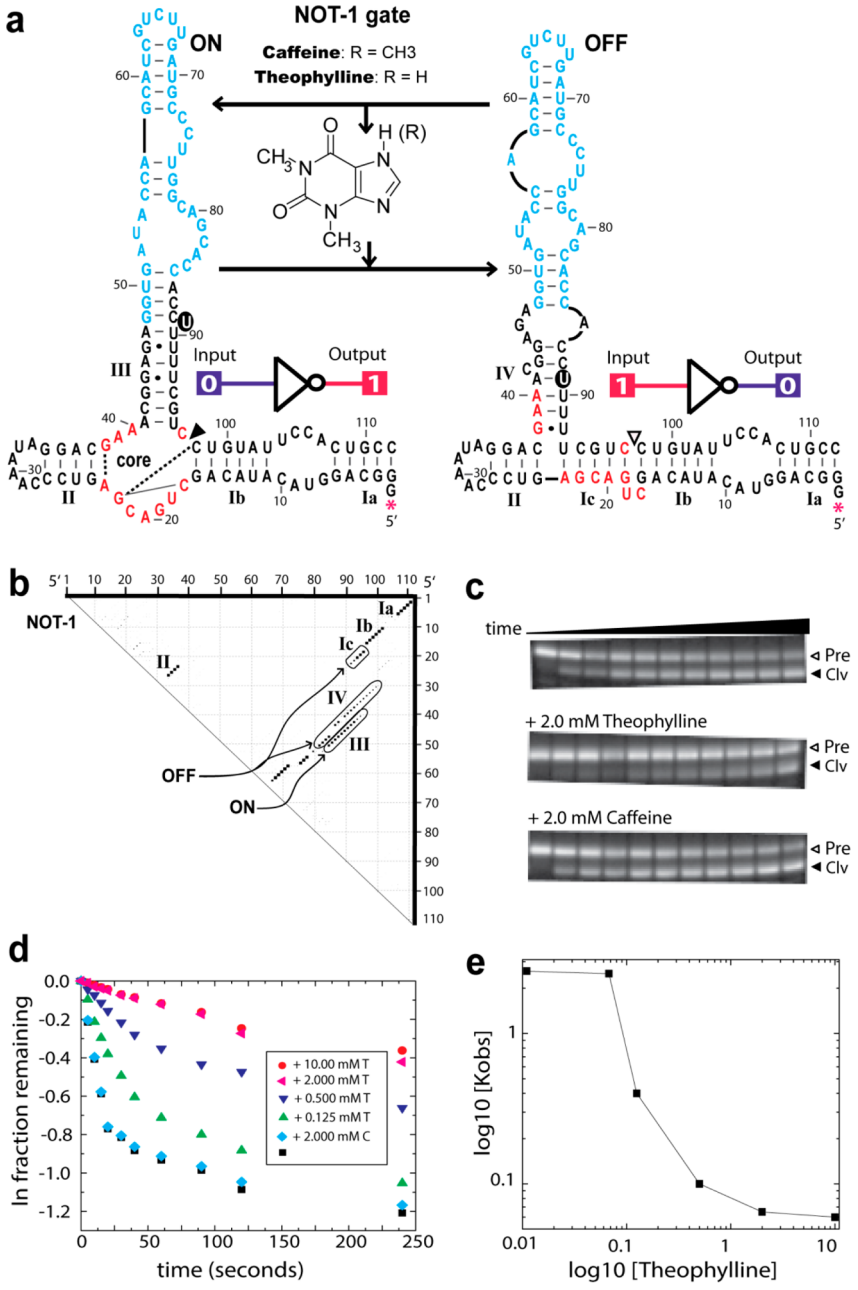

Figure 2. Characterization of a NOT-1 theophylline-sensing riboswitch. (a) An allosteric ribozyme with a NOT logic function based on the extended hammerhead sequence that senses theophylline and exhibit high-speed of self-cleavage under low Mg^{2+} concentration. (b) A dot matrix plot is shown wherein larger points reflect greater probability of base pairing. Encircled points reflect the main differences between the OFF (stem IV) and ON (stem II) states. Nucleotides 1 through 112 are numbered from 5′ to 3′ across the top and right of the plots. Note that both ON and OFF: states are formed as the inactive state is a bit more stable. (c) The allosteric ribozyme (5′-TAMRA-labeled, Pre), depicted in Figure 1, undergoes fast self-cleavage in the absence of theophylline and the resulting cleavage fragment (Clv) is separated from the precursor by denaturing. The products were visualized, and cleavage yields were quantified. The reaction was conducted at 37 °C in physiological-like buffer conditions. Selective deactivation of ribozyme self-cleavage in the presence of 2.0 mM theophylline is demonstrated in second gel image. The third gel images of the kinetics of ribozyme self-cleavage in the presence of 2.0 mm caffeine shows no effect. (d) Plot using data derived from various theophylline and caffeine concentrations depicts the natural logarithm of the fraction of RNA remaining (noncleaved) vs time. (e) The plot depicts K_{obs} of ribozyme self-cleavage vs corresponding theophylline concentrations.

from the partition function. If stem IV is more dominant than 20%, then reject the sequence and go to 1.1; otherwise, save the sequence and go to 1.1.

2.1 Using the secondary structure generated by the stage 1 of the algorithm. Run the program RNAinverse (Vienna RNA folding package) program to generate a new RNA sequence that possesses similar secondary structure folding by randomizing the X nucleotides (Figure 1c,d).

2.2 Determine whether stem III (Figure 1d, ON state) of the ribozyme is formed using the probability dot matrix plot derived from the partition function. If stem III is not present reject the sequence and go to 2.1. If stem III is present, then register the candidate sequence and go to the next step.

2.3 Determine whether stem IV (Figure 1d, OFF state) of the ribozyme is formed using the probability dot matrix plot derived from the partition function. If stem IV is not present,

dx.doi.org/10.1021/bm400299a | *Biomacromolecules* 2013, 14, 1240−1249

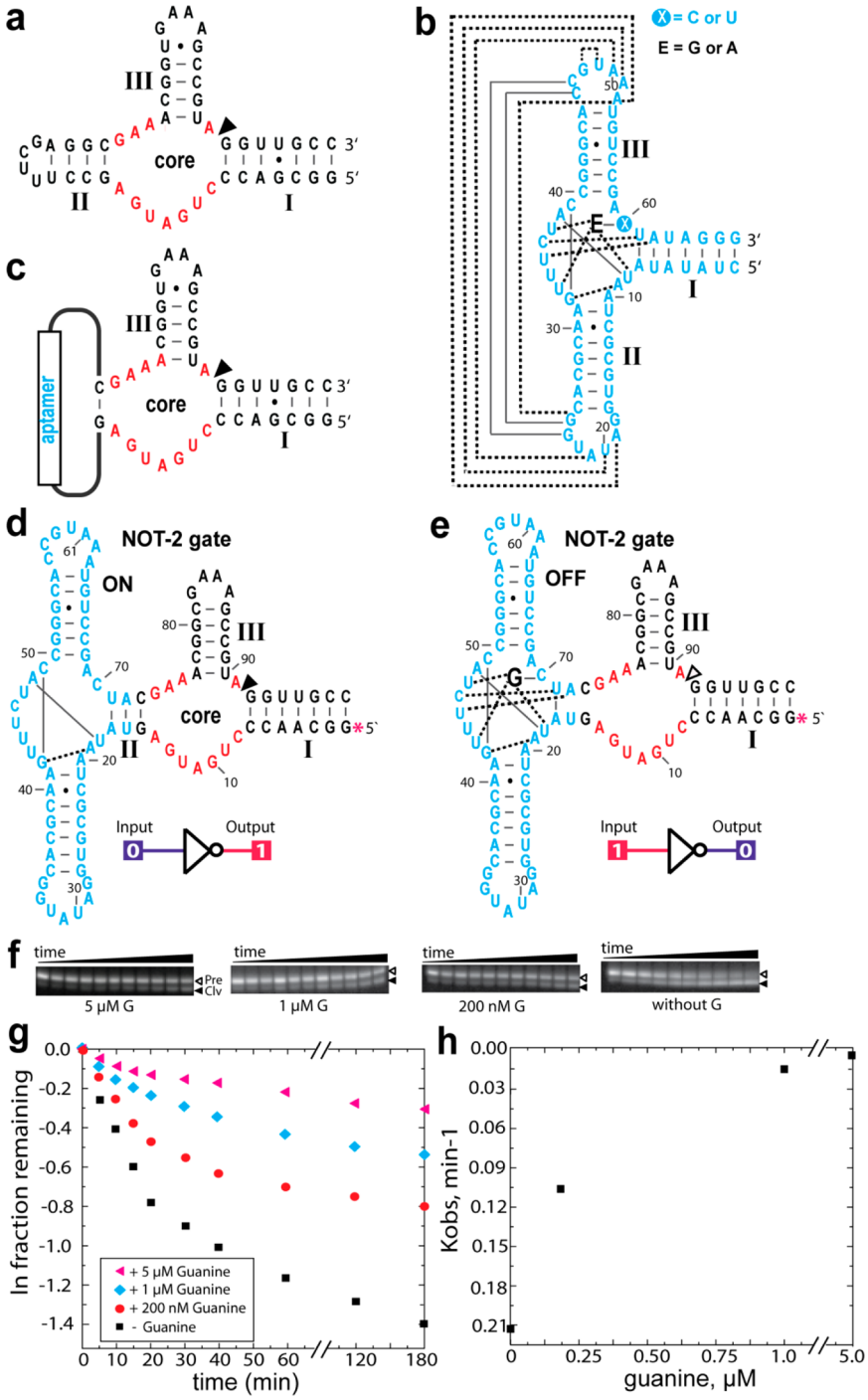

Figure 3. Allosteric ribozyme with NOT Boolean function obtained by the fusing of the hammerhead ribozyme with guanine aptamer. (a) The minimal version of the hammerhead ribozyme has three stems (from I to III) and unpaired nucleotides of the core (red). The cleavage site of the ribozyme is indicated by an arrowhead. (b) An example of the purine aptamer, found in 13 human bacterial pathogens, is depicted. The aptamer has three stems. In addition to the secondary structure, all canonical (solid lines) and noncanonical (dashed lines) interactions of the tertiary structure are depicted. The X nucleotide (at the 60th position) can be either C for the guanine or U for the adenine aptamer. The effector (E) can be either guanine, for which all tertiary interactions are given, or adenine. (c) The allosteric domain is embedded into stem II. This domain is an RNA aptamer that selectively binds small molecules. (d) An allosteric ribozyme with a NOT logic function that sense guanine is depicted. The hammerhead ribozyme is fused with a guanine aptamer (blue). In the absence of guanine, the ribozyme is in an active state and cleaves itself in the position indicated by the arrowhead. The red star (*) indicates TAMRA-labeling. (e) When guanine is present, it binds to the aptamer domain (blue) with the various canonical (solid lines) and noncanonical (dashed lines) interactions. This results in disturbing stem II that switches the ribozyme into an inactive state. (f) Gel images of cleavage kinetics with the NOT-2 ribozyme in various concentrations of guanine are shown. (g) The cleavage kinetics established from the gel images in the previous section is plotted as a natural logarithm of fraction remaining (noncleaved) vs time. (h) The plot depicts K_{obs} of ribozyme self-cleavage vs corresponding guanine concentrations.

dx.doi.org/10.1021/bm400299a | *Biomacromolecules* 2013, 14, 1240−1249

reject the sequence and go to 2.1. If stem IV is present, then register the candidate sequence and go to the next step.

2.4 Compare the possibility of forming stems III and IV (Figure 1d, OFF state) of using the probability dot matrix plot derived from the partition function. If stem IV is more dominant than 10%, then reject the sequence and go to 2.1. Otherwise, save the sequence and go to 2.1.

Design of RNA Switches by Modeling 3D Interactions. For modeling 3D interactions between the guanine and its RNA aptamer, I used the tertiary structure (NDB ID: NA1833) from the protein data bank (http://www.pdb.org/) and the Amber suite (http://amber.script.edu/) that allows us to carry out molecular dynamics simulations on our purine sensors. I basically used the force fields that are in the public domain to calculate some interactions between the guanine and some aptamer nucleotides that are embedded into stem II of the ribozymes (Figures 3 and S3).

RNA Synthesis. Synthetic DNA oligomers were purchased from Integrated DNA Technology (Leuven, Belgium). All DNAs were purified by denaturing (8 M urea) PAGE before use. Double-stranded (ds) DNAs for in vitro transcription were prepared by overlap extension using SuperScript II reserve transcriptase (Invitrogen, Carlsbad, CA) in a reaction volume of 50 μL according to the manufacturer's instructions. DNA oligomers corresponding to the nontemplate strand carried a T7 RNA promoter sequence (TAATACGACTCACTATA). The dsDNAs obtained were precipitated with ethanol and used as templates for transcription in vitro (RiboMax, Promega, Madison, WI) in the presence of either 5′-TAMRA-ApG or 5′-Biotin-ApG (IBA, Göttingen, Germany) according to the manufacturer's instructions. The transcribed RNAs, produced during a 3 h long incubation, were isolated by using denaturing 6% PAGE and recovered from the gel by the crash and soak procedure.

Allosteric Ribozyme Assays. The extended hammerhead ribozymes were added in a reaction solution containing 100 mM HEPES, (pH 7.5 at 37 °C), 25 mM NaCl, and 1 mM $MgCl_2$ at 37 °C. Reactions were terminated by the addition of an equal volume of gel loading buffer containing 200 mM EDTA

Allosteric switches based on the minimal version of the hammerhead ribozyme (200 nM) were incubated in a solution containing 50 mM Tris-HCl with pH 8.5 at 24 °C and 20 mM $MgCl_2$. Ribozyme reactions were initiated by adding target RNA molecules (typically to a final concentration of 80 nM) at 24 °C.

Rate constants were determined by plotting the natural logarithm of the fraction of RNA remaining noncleaved versus time, wherein the negative slope of the resulting line reflects k_{obs}. The reaction products were run on 6% denaturing PAGE. The 5′-TAMRA-labeled RNAs from the gels were detected using a blue-light transilluminator, DarkReader-195 M from Clare Chemical Research, Inc. (Dolores, CO) and Nikon D5100 digital camera (Nikon Imaging Japan Inc., Tokyo, Japan) equipped with a 520 nm optical filter. The images were analyzed with the ImageJ software (NIH, Bethesda, MD). All small molecules are purchased from Sigma-Aldrich.

To detect a cleavage of external substrates by the purine-sensing ribozymes, target RNA was used that is 5′-end Cy3-labeled and FAM and at the 3′-end. The kinetic was determined by the increment of the fluorescence signal of FAM upon cleavage measured at 520 nm. Biotin-labeled RNAs were immobilized to streptavidin-coated magnetic beads (Dynabeads, Invitrogen, Carlsbad, CA) as described by the manufacturer.

RESULTS

Design and Characterization of High-Speed Theophylline-Sensing Ribozymes with NOT Logic Function. An extended version of hammerhead ribozyme (Figure 1a) from *Schistosoma mansoni* was used as a parental construct for the design of ribozymes that are deactivated by allosteric interactions with theophylline. These designer ribozymes are intended to have fast cleavage kinetics under physiologically relevant conditions.

The hammerhead ribozyme from *Schistosoma mansoni* exhibits improved function because it forms a tertiary structure between the loop sequences of stem II and a bulge loop within stem I (Figure 1a). To preserve these important 3D interactions between stems I and II, I have embedded the theophylline aptamer (Figure 1b) into stem III for the design of constructs that function as NOT gates (Figure 1d). As a result, these critical ribozyme tertiary interactions are not disrupted (Figure 1a), and the designer ribozymes can exhibit fast cleavage kinetics. I employed computational selection of allosteric ribozymes with a NOT Boolean logic function (Figure 1c) by randomizing the nucleotides that connect the aptamer with stem III of the ribozyme (Figure 1d). The procedure computes RNA secondary structures using partition function for RNA folding in combination with a random search algorithm as detailed in Materials and Methods.

The obtained design, termed NOT-1 (Figure 2a), is predicted to form both stems III and IV with a different possibility shown on the dot matrices (Figure 2b). This is done because the free energy released upon theophylline binding to the RNA aptamer is much smaller than that released by hybridization of 22mer DNA to the allosteric domain of oligonucleotide-sensing ribozymes.[11] Therefore, there should be a very tight balance between the ON (stem III) and the OFF (stem IV) states of the ribozyme. If the stem III is very dominant, then the ribozyme will cleave itself at the highest speed but it will not be responsive to theophylline. In contrast, if stem IV is very dominant, then the ribozyme will cleave itself relatively slow and may not be suitable for *in vivo* applications. I probe these assumptions using the theophylline aptamer in our designer ribozymes because it has been proven that can work in the cell.[10] In addition, theophylline has been used as a medicine.

The NOT-1 construct works is predicted to self-cleave in the absence of theophylline. Therefore, the preparation of the RNA is expected to pose a problem because the ribozyme will undergo self-cleavage during transcription in vitro. To avoid this outcome, DNA templates corresponding to the NOT-1 RNA were transcribed in the presence 10 μM of the antisense oligonucleotide TATTTGGACCTCATCAGC. However, the NOT-1 ribozyme has exhibited about 20% self-cleavage when produced by in vitro transcription under these conditions.

The ribozyme exhibits robust self-cleavage activity ($k_{obs} \sim 1.3$ min^{-1}) when incubated in the absence of effector and $k_{obs} \sim 0.04$ min^{-1} in the presence of 2 mM theophylline (Figure 2c). This makes ~30-fold dynamic range between ON and OFF state. An addition of theophylline causes significant inhibition of the NOT-1 ribozyme. Four different concentrations of theophylline have been tested for inhibition of NOT-1 ribozyme (Figure 2d). As a result, I established $K_d \sim 100$ μM for the NOT-1 ribozyme binding theophylline (Figure 2e). In contrast, the ribozyme was completely active in the presence of 2 mM caffeine (Figure 2c), which differs with theophylline in a single methyl group (Figure 2a). This can be explained with the fact that the aptamer is very specific for theophylline and does not respond to caffeine.

Using the second part of the algorithm, I obtained two additional NOT ribozyme sequences. I try to optimize the NOT-1 ribozyme in two different directions. In the first way, I stabilized stem III of the NOT-3 ribozymes for the expense of stem IV (Figure S1a,b). As expected, the NOT-3 ribozyme

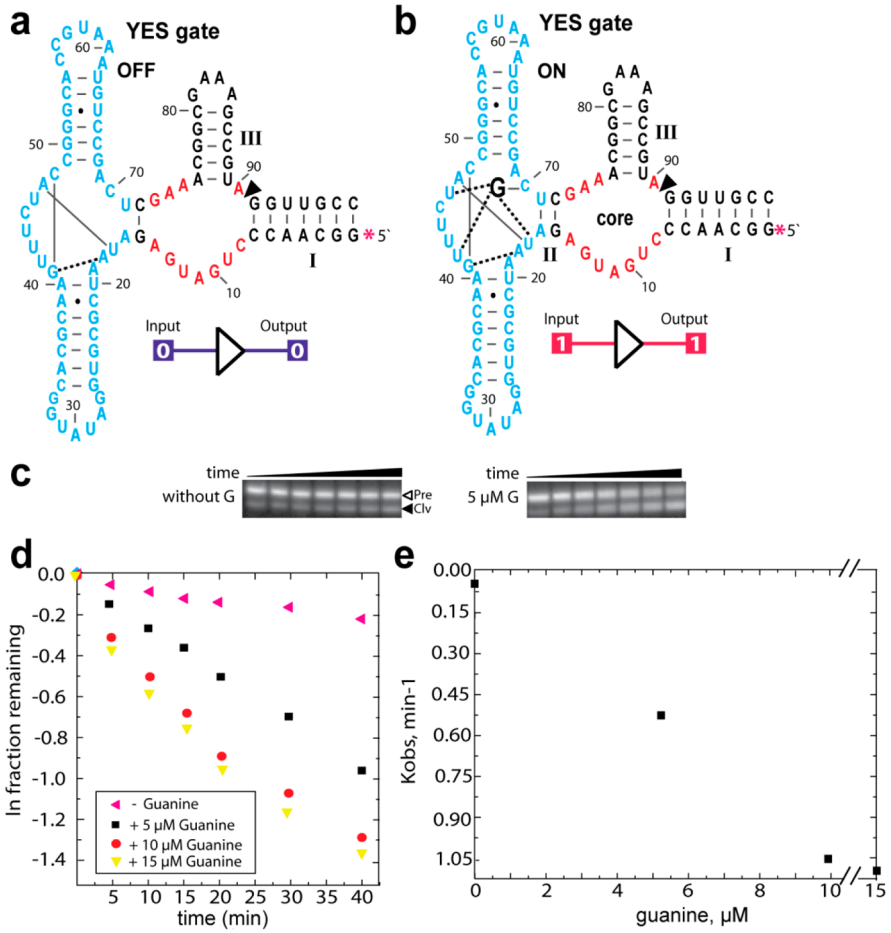

Figure 4. An allosteric ribozyme with a YES logic function that senses guanine. (a) In the absence of guanine, the ribozyme folds into an inactive state because the stem II is not properly formed. (b) In contrast, when guanine is present, it binds to the aptamer domain (blue) via various canonical (solid lines) and noncanonical (dashed lines) interactions. As a result, stem II is formed and the ribozyme turns into an active state. (c) Gel images of cleavage kinetics with the YES ribozyme in various concentrations of guanine are shown. (d) The kinetics of cleavage established from the gel images in the previous section is plotted as a natural logarithm of fraction remaining (noncleaved) vs time. (e) The plot depicts K_{obs} of ribozyme self-cleavage vs corresponding guanine concentrations.

exhibited faster kinetics of cleavage ($k_{obs} \sim 2$ min^{-1}) than that of NOT-1. However, the NOT-3 ribozyme is less responsive to theophylline (Figure S1c) than NOT-1. In contrast, the NOT-4 ribozyme was designed to have stem IV more stable than stem III (Figure 2Sa,b). This results in slower cleavage kinetics ($k_{obs} \sim 0.4$ min^{-1}) than the NOT-1 (Figure 2Sc). This makes us believe that the NOT-1 ribozyme is close to the optimal sequence.

The use of partition function for RNA folding computes all possible secondary structures, which is much more accurate than that based on the minimal free energy based on one secondary structure only. One RNA sequence can fold at the same time in several different secondary structures with close thermodynamic stability. In addition, by testing all possible base substitutions of the communication module with a certain length between the ribozyme and the allosteric domain, I have increased the change to find RNA sequences with the desired properties.

I have decided to engineer high-speed ribozymes with a NOT logic function because they can be used to switch on the expression exogenous genes in the cell in the presence of specific RNA molecules. This may be used as a novel gene therapy tool. In contrast, high-speed ribozymes with a YES logic function can switch off the expression exogenous genes in the cell when the specific effector is present, which is less useful.

Design and Validation of Purine-Sensing Ribozymes with NOT or YES Logic Functions. I have engineered allosteric ribozymes with a NOT or YES logic function that sense purines (guanine or adenine) employ molecular modeling. The designer ribozymes are based on the minimal version of the hammerhead ribozyme (Figure 3a) fused with a purine aptamer (Figure 3b) that is a part of bacterial riboswitches. There are three subclasses: for guanine, adenine, and 2-deoxyguanosine.[20] The purine aptamers (Figure 3b) share common secondary and tertiary structures and differ mainly in some single nucleotide substitutions. The essential single nucleotide substitution, which alters the specificity of the aptamer, is termed as X at the 60th position in Figure 3b. If cytosine is at this position, the aptamer is specific for guanine. If uracil resides at the 60th position, the aptamer will bind adenine. The 3D structure of the purine aptamers in the presence of effectors has been already solved.[25] All canonical and noncanonical interactions of the guanine aptamer are depicted in Figure 3b. Based on these interactions, I fused the purine aptamers to the hammerhead ribozyme at stem II (Figure 3c).

dx.doi.org/10.1021/bm400299a | Biomacromolecules 2013, 14, 1240−1249

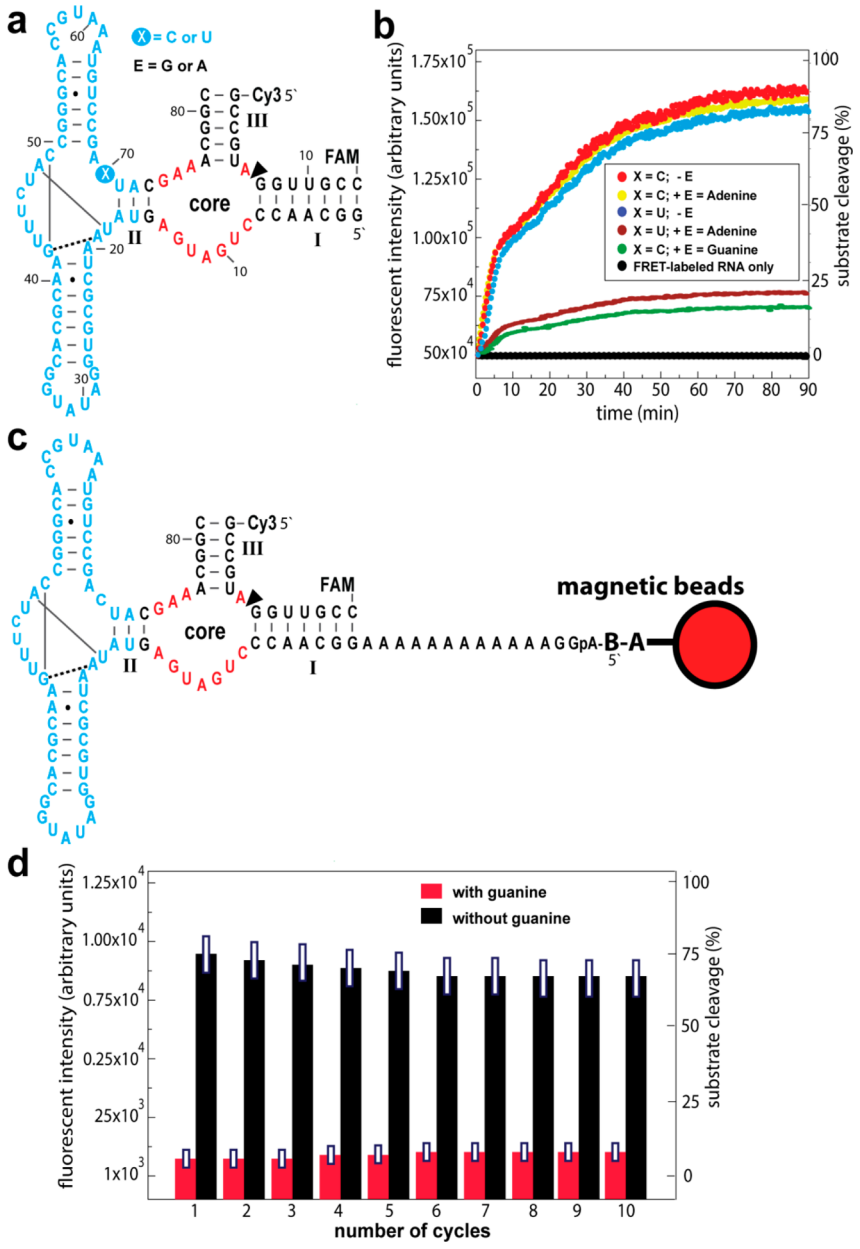

Figure 5. High-throughput compatible arrays based on guanine sensing NOT-2 ribozyme. (a) The NOT-2 ribozyme is modified to cleave an external RNA molecule. The substrate RNA is Cy3- and FAM-labeled, respectively, at the 5′ to 3′ ends. Therefore, the external RNA serves as a FRET pair. In addition, the aptamer domain is modified by a single base substitution at the 70th position (X). If the base is cytosine, the aptamer will bind guanine while the X is uracil it will sense adenine. (b) Cleavage kinetics of the FRET RNA by the guanine and the adenine sensing ribozymes, shown in the previous section, is plotted. Both effectors when present were at a concentration of 5 μM. (c) The NOT-2 ribozyme is immobilized to strepavidin-coated magnetic beads. (d) Fluorescent intensity values of 10 consecutive cycles on magnetic beads with immobilized NOT-2 ribozyme. In the absence of guanine (the black bars), the ribozyme cleaves its substrate FRET-labeled RNA. In the presence of 5 μM guanine, the ribozyme function is inhibited. Both experiments are performed for 15 min.

In contrast to the extended version (Figure 1a), the minimal version of the hammerhead ribozyme does not have a bulge loop in stem I (Figure 3a). This avoids interactions between the bulge loop in stem I and the loop in stem II. As a result, the minimal version of the hammerhead ribozyme reaches its highest speed of cleavage at much higher concentration of Mg^{2+} (20 mM) than the extended ribozyme (1 mM).

In the absence of guanine, the ribozyme with NOT logic function is designed to fold into an active state, where all three stems are formed (Figure 3d). As a result, the ribozyme NOT-2 is supposed to cleave, where indicated by the arrowhead (Figure 3d). When guanine is present, it binds to the aptamer domain with various canonical and noncanonical bounds (Figure 3e). Consequently, the guanine aptamer is folded as two noncanonical base pairs are formed between nucleates at positions 46 and 71 and nucleates at the positions 45 and 72. It results in the disturbance of stem II that is supposed to inhibit the cleave−cleavage of the ribozyme modeling, the 3D interactions with molecular dynamics simulations (blue, Figure 3e).

I have tested the kinetics of ribozyme self-cleavage in four different concentrations of guanine as described in Materials

dx.doi.org/10.1021/bm400299a | *Biomacromolecules* 2013, 14, 1240−1249

and Methods. The gel images are shown in Figure 3f while the results of them are plotted as a natural logarithm of fraction remaining versus time in Figure 3g. Based on these results, I have estimated K_{obs} for the NOT-2 ribozyme various concentrations of guanine (Figure 3h). The K_{obs} in the absence of guanine is 0.2 min^{-1}, while in the presence of 5 μM guanine is 0.006 min^{-1} binding guanine. This 33-fold difference represents a sufficient dynamic range for applying this ribozyme as a sensor for testing small molecules for specific binding to the guanine aptamer. Based on these results, I estimated K_d = 500 NM for binding guanine of the NOT-2 ribozyme. The K_d of the guanine aptamer alone is about 5 nM.

In addition, I describe a guanine-sensing ribozyme with a YES logic function (Figure 4). This ribozyme differs with the NOT-2 in the absence of one base pair (U-A) only in stem II. As a result, stem II is destabilized in the absence of guanine, and the self-cleavage of the ribozyme is significantly slowed down (Figure 4a). In contrast, upon guanine binding, stem II is formed as modeled by 3D interactions with molecular dynamics simulations (Figure 4b). Consequently, the ribozyme's cleavage is speeded up. In contrast to the NOT-2 ribozyme (Figure 3b), the noncanonical U-C is not supposed to form because the absence of U-A (Figure 4b) noncanonical integration, as computed by the force fields. Gel images of ribozyme's self-cleavage in the presence and absence of guanine are shown in Figure 4c while the results are depicted in Figure 4d. I estimate K_d = 5 μM for the YES ribozyme (Figure 4e). The K_{obs} of the YES ribozyme in the presence of 5 μM guanine is 0.1 min^{-1} and 0.005 min^{-1} in the absence of effector, which makes a difference of 20-fold. This dynamic range is sufficient for the YES ribozyme to be successfully employed as a biosensor in vitro.

The K_d of the YES ribozyme is about 10-fold higher than that of the NOT-2. This can be explained with the fact that stabilization of stem II of NOT-2 requires a higher concentration of guanine than that for destabilization of stem II of the YES ribozyme. This should be taken into account when using this ribozyme, a biosensor, in vitro when testing different effectors at a concentration around or a bit higher than that of K_d.

High-Throughput Compatible Arrays. Most of the riboswitches discovered up to now are built of an aptamer domain and an expression platform. I can easily identify the aptamer part, which is responsible for ligand binding using RNA biochemical methods such as inline probing. However, such an approach is not scalable to HTS settings because it requires manually running polyacrylamide gel electrophoresis (PAGE) gels. HTS arrays can include riboswitch-based sensors that can report binding of analogs of the original effectors. Such molecular sensors can be engineered to cleave external RNAs. This approach gives us several major benefits. First of all, I can employ a fluorescence resonance energy transfer (FRET) pair to the substrate RNAs. That will enable us to detect cleave in a solution on microtiter plates. This is fully scalable to HTS and can follow the cleavage kinetics in real time. I can use the designer sensors under multiple turnover conditions, which amplifies the signal over time.

To make HTS compatible arrays, I have engineered the allosteric ribozymes to cleave external FRET-labeled RNA molecules, as demonstrated in Figure 5a. The substrate RNA was 5′-terminus Cy3 (a fluorochrome) and 3′-terminus FAM (a quencher) labeled. The aptamer domain (blue, Figure 5a) differs in a single nucleotide at the 70th position that can be either cytosine (C) for the guanine or uracil (U) for the adenine aptamers.

The real time cleavage kinetics of FRET-labeled RNA is depicted in Figure 5b. The results obtained are consistent with the specific binding expected for guanine and adenine. In the absence of effectors, both ribozymes are in an active conformation (the red and blue lines, Figure 5b). In the presence of specific effectors (5 μM either G or A), the ribozymes are turned into inactive conformations as the guanine ribozyme (the green line, Figure 5b) is slightly more inhibited than that of the adenine-sensing ribozyme (the brown line, Figure 5b). This can be explained with the fact that guanine binds its aptamer stronger than the adenine. Note that the guanine-sensing ribozyme is not inhibited by adenine (the yellow line, Figure 5b). These experiments can be easily done under multiple turnover conditions by raising the temperature. This will amplify the signal. The businesses presented can be easily used in an HTS formant for the discovery of small molecules that bind specifically adenine or guanine aptamers.

The purine riboswitches are found in 13 different human pathogenic bacteria. Therefore, the development of various HTS methods for purine riboswitches is of certain interest not only to academic researchers but also to the pharmaceutical industry.[26]

Here I demonstrate a high-throughput compatible array using the guanine-sensing NOT-2. All RNA molecules were biotinylated at their 5′-terminus as described in Materials and Methods. That was used to immobilize these RNAs to streptavidin-coated magnetic beads as detailed in Materials and Methods (Figure 5c). To avoid any steric problems to RNA hybridization with the ribozyme I used a spacer built of 12 adenine nucleotides.

I have made 10 consecutive cycles on 1 mg beads (Figure 5d). Each cycle consists of two steps for 15 min. In the first step, the immobilized with RNA beads were incubated in the presence of 5 μM guanine and 1 μM FRET-labeled substrate RNA at 25 °C in a final volume of 20 μL in 96 well microplates (Corning, Inc.). Fluorescent images were taken with a Nikon 5100 digital camera equipped with a fluorescence filter that passes light above 500 nm and analyzed by ImageJ software. As a light source, I used a blue-light transilluminator, DarkReader-195 M (light length from 400 to 500 nm) from Clare Chemical Research, Inc. The same experiments were carried out in the absence of guanine. The results obtained (Figure 5d) suggest that I can use our ribozymes immobilized on beads for multiple cycles of HTS assays for small molecules that specifically bind to purine aptamers for antibacterial drug discovery. Moreover, I have already successfully used the guanine ribozyme immunized on beads in HTS settings. These results will be published elsewhere.

■ DISCUSSION

The presented approach for computational selection of small molecule-sensing riboswitches based on modeling secondary structures uses the partition function for RNA folding like the already published computational design of oligonucleotide-sensing ribozymes.[11] Both computational methods are very time efficient, computing many different sequences (from hundreds of thousands to over several millions) using random search algorithms. However, the selection criteria in these two methods are completely distinct.

When we designed an oligonucleotide sensing allosteric ribozymes, the difference in thermodynamic stability between

the OFF and ON states is at least 8 kcal mol^{-1}. In contrast, when we engineered a small molecule-sensing ribozyme, this difference was much smaller. In addition, they use different dataflow schemes having different effectors. I have embedded the theophylline aptamer in stem III of the extended version of the hammerhead ribozyme. Thus, I have preserved all tertiary interactions between stems I and II that are important for the fast kinetics of ribozyme's self-cleavage. As a result, our theophylline-sensing ribozymes are high-speed molecular switches that work under physiologically relevant conditions. The second main reason for the fidelity of our approach is the application of the partition function for RNA folding that computes not just one but all possible secondary structures using a dynamic programming algorithm. The dynamic programming algorithms are computationally very efficient. Therefore, I can fold a large number of different RNA sequences in for several min on an average personal computer. Note that I can change the number of randomized (N) nucleotides between stem III and the aptamer. As a result, I can obtain allosteric ribozymes with different properties such as cleavage kinetics and a dynamic range of allosteric activation.

The designer ribozymes presented have at least a 25-fold dynamic range between ON and OFF states, which is sufficient for most in vivo and in vitro applications. The ribozymes are very specific to their ligands. All designer ribozymes tested in this study are rapid switches. This means that they can be activated or deactivated at any time after adding a specific effector.

In contrast, high-speed allosteric ribozymes obtained by in vitro selection cannot be switched by the effector after being folded.[27] Such ribozymes can function only when they fold in the presence of the effector. If the effector is added after their folding, these ribozymes cannot alter their function at all. To switch in a solution after synthesis, these ribozymes have to be heated up for denaturing their structures and cold down in the presences of effector. Therefore, they have limited applications as biosensors, especially in the cell. Through the NOT logic function I can turn on exogenous gene expression in eukaryotes in the presence of a effector moleculer.[28]

In contrast to other modeling approaches that manually test the effect of some base substitutions on the 3D structure, I used a random search algorithm to automatically compute the result of all intended base substitutions on the structure as depicted on Figure S3. We have to know the tertiary structure of the aptamer with a bound ligand to apply modeling of 3D interactions. If this information is not available, I have to use computational designs based on the modeling secondary structures. In addition, if the 3D interactions are more than a dozen, it can be difficult to compute all of them. In our case, I computed only two 3D interactions that alternate in the presence of the ligand.

CONCLUSIONS

The presented computational approaches for designing small molecule-sensing allosteric ribozymes are proven to be accurate and time-efficient in producing molecular biosensors with diverse properties. These ribozymes can be used for both various in vitro and in vivo applications. The three-dimensional modeling approach is applicable to 90% of the known bacterial riboswitches since they have solved 3D-structures of their aptamer domains. As demonstrated for the purine aptamers, I can engineer allosteric ribozymes by fusing an aptamer domain of a riboswitch to the minimal version of the hammerhead ribozyme. Such ribozymes can be used as biosensors for many different HTS arrays for antibacterial drug discovery. This can be a valuable approach since bacterial riboswitches are found most human pathogenic bacteria. Therefore, some riboswitches are promising new targets for antibacterial drug discovery. In addition, the small-molecules allosteric ribozymes can be used for molecular computing as well as for detection of small molecules in a solution.[8]

The theophylline-sensing ribozymes can be used to regulate gene expression both in pro-and eukaryotes. An important advantage of the designs generated by these computational approaches is that aptamers can be treated as tunable modules, which makes possible the generation of large numbers of ribozymes with tailored functions by making only a few changes. This modularity can be exploited to produce rapidly variant RNA switches that exhibit distinct effector specificities compared to the use of in vitro selection, which might have to be repeated for each new target ligand.

ASSOCIATED CONTENT

Supporting Information

Additional supporting figures. This material is available free of charge via the Internet at http://pubs.acs.org.

AUTHOR INFORMATION

Corresponding Author

*E-mail: robert.penchovsky@hotmail.com. Phone/Fax: +35928167340.

Notes

The authors declare no competing financial interest.

ACKNOWLEDGMENTS

This research is funded by Grant DDVU02/5/2010 awarded by the Bulgarian National Science Fund (BNSF). I thank Czvetelina C. Stoilova, Sofia University, for assistance with some experiments.

REFERENCES

(1) Vinkenborg, J. L.; Karnowski, N.; Famulok, M. Aptamers for allosteric regulation. *Nat. Chem. Biol.* **2011**, *7* (8), 519−27.

(2) Ellington, A. D.; Szostak, J. W. In vitro selection of RNA molecules that bind specific ligands. *Nature* **1990**, *346* (6287), 818−22.

(3) Liu, J.; Cao, Z.; Lu, Y. Functional nucleic acid sensors. *Chem. Rev.* **2009**, *109* (5), 1948−98.

(4) Breaker, R. R. Natural and engineered nucleic acids as tools to explore biology. *Nature* **2004**, *432* (7019), 838−45.

(5) (a) Winkler, W. C.; Cohen-Chalamish, S.; Breaker, R. R. An mRNA structure that controls gene expression by binding FMN. *Proc. Natl. Acad. Sci. U.S.A.* **2002**, *99* (25), 15908−13. (b) Mironov, A. S.; Gusarov, I.; Rafikov, R.; Lopez, L. E.; Shatalin, K.; Kreneva, R. A.; Perumov, D. A.; Nudler, E. Sensing small molecules by nascent RNA: a mechanism to control transcription in bacteria. *Cell* **2002**, *111* (5), 747−56. (c) Mandal, M.; Breaker, R. R. Gene regulation by riboswitches. *Nat. Rev. Mol. Cell Biol.* **2004**, *5* (6), 451−63.

(6) (a) Mandal, M.; Boese, B.; Barrick, J. E.; Winkler, W. C.; Breaker, R. R. Riboswitches control fundamental biochemical pathways in Bacillus subtilis and other bacteria. *Cell* **2003**, *113* (5), 577−86. (b) Winkler, W. C.; Breaker, R. R. Regulation of bacterial gene expression by riboswitches. *Annu. Rev. Microbiol.* **2005**, *59*, 487−517. (c) Breaker, R. R. Complex riboswitches. *Science* **2008**, *319* (5871), 1795−7.

(7) Blount, K. F.; Breaker, R. R. Riboswitches as antibacterial drug targets. *Nat. Biotechnol.* **2006**, *24* (12), 1558−64.

(8) Seetharaman, S.; Zivarts, M.; Sudarsan, N.; Breaker, R. R. Immobilized RNA switches for the analysis of complex chemical and biological mixtures. *Nat. Biotechnol.* **2001**, *19* (4), 336−41.
(9) Blount, K.; Puskarz, I.; Penchovsky, R.; Breaker, R. Development and application of a high-throughput assay for glmS riboswitch activators. *RNA Biol.* **2006**, *3* (2), 77−81.
(10) Win, M. N.; Smolke, C. D. Higher-order cellular information processing with synthetic RNA devices. *Science* **2008**, *322* (5900), 456−60.
(11) Penchovsky, R.; Breaker, R. R. Computational design and experimental validation of oligonucleotide-sensing allosteric ribozymes. *Nat. Biotechnol.* **2005**, *23* (11), 1424−33.
(12) Piganeau, N.; Thuillier, V.; Famulok, M. In vitro selection of allosteric ribozymes: theory and experimental validation. *J. Mol. Biol.* **2001**, *312* (5), 1177−90.
(13) (a) Tang, J.; Breaker, R. R. Rational design of allosteric ribozymes. *Chem. Biol.* **1997**, *4* (6), 453−9. (b) Amontov, S.; Jaschke, A. Controlling the rate of organic reactions: rational design of allosteric Diels-Alderase ribozymes. *Nucleic Acids Res.* **2006**, *34* (18), 5032−8. (c) Liang, J. C.; Smolke, C. D. Rational design and tuning of ribozyme-based devices. *Methods Mol. Biol.* **2012**, *848*, 439−54.
(14) (a) Scott, W. G.; Murray, J. B.; Arnold, J. R.; Stoddard, B. L.; Klug, A. Capturing the structure of a catalytic RNA intermediate: the hammerhead ribozyme. *Science* **1996**, *274* (5295), 2065−9. (b) Scott, W. G. Crystallographic analyses of chemically synthesized modified hammerhead RNA sequences as a general approach toward understanding ribozyme structure and function. *Methods Mol. Biol.* **1997**, *74*, 387−91.
(15) Penchovsky, R. Engineering integrated digital circuits with allosteric ribozymes for scaling up molecular computation and diagnostics. *ACS Synth. Biol.* **2012**, *1*, 18.
(16) Osborne, E. M.; Schaak, J. E.; Derose, V. J. Characterization of a native hammerhead ribozyme derived from schistosomes. *RNA* **2005**, *11* (2), 187−96.
(17) Zimmermann, G. R.; Wick, C. L.; Shields, T. P.; Jenison, R. D.; Pardi, A. Molecular interactions and metal binding in the theophylline-binding core of an RNA aptamer. *RNA* **2000**, *6* (5), 659−67.
(18) Batey, R. T.; Gilbert, S. D.; Montange, R. K. Structure of a natural guanine-responsive riboswitch complexed with the metabolite hypoxanthine. *Nature* **2004**, *432* (7015), 411−5.
(19) Penchovsky, R.; Stoilova, C. C. Riboswitch-based antibacterial drug discovery using high-throughput screening methods. *Expert Opin. Drug Discovery* **2013**, *8* (1), 65−82.
(20) (a) Kim, J. N.; Breaker, R. R. Purine sensing by riboswitches. *Biol. Cell* **2008**, *100* (1), 1−11. (b) Jain, N.; Zhao, L.; Liu, J. D.; Xia, T. Heterogeneity and dynamics of the ligand recognition mode in purine-sensing riboswitches. *Biochemistry* **2010**, *49* (17), 3703−14.
(21) Penchovsky, R.; Ackermann, J. DNA library design for molecular computation. *J. Comput. Biol.* **2003**, *10* (2), 215−29.
(22) McCaskill, J. S. The equilibrium partition function and base pair binding probabilities for RNA secondary structure. *Biopolymers* **1990**, *29* (6−7), 1105−19.
(23) Mathews, D. H.; Sabina, J.; Zuker, M.; Turner, D. H. Expanded sequence dependence of thermodynamic parameters improves prediction of RNA secondary structure. *J. Mol. Biol.* **1999**, *288* (5), 911−40.
(24) Gruber, A. R.; Lorenz, R.; Bernhart, S. H.; Neubock, R.; Hofacker, I. L. The Vienna RNA websuite. *Nucleic Acids Res.* **2008**, *36* (Web Server issue), W70−4.
(25) Serganov, A.; Yuan, Y. R.; Pikovskaya, O.; Polonskaia, A.; Malinina, L.; Phan, A. T.; Hobartner, C.; Micura, R.; Breaker, R. R.; Patel, D. J. Structural basis for discriminative regulation of gene expression by adenine- and guanine-sensing mRNAs. *Chem. Biol.* **2004**, *11* (12), 1729−41.
(26) (a) Kim, J. N.; Blount, K. F.; Puskarz, I.; Lim, J.; Link, K. H.; Breaker, R. R. Design and antimicrobial action of purine analogues that bind guanine riboswitches. *ACS Chem. Biol.* **2009**, *4* (11), 915−27. (b) Villa, A.; Wohnert, J.; Stock, G. Molecular dynamics simulation study of the binding of purine bases to the aptamer domain of the guanine sensing riboswitch. *Nucleic Acids Res.* **2009**, *37* (14), 4774−86. (c) Daldrop, P.; Reyes, F. E.; Robinson, D. A.; Hammond, C. M.; Lilley, D. M.; Batey, R. T.; Brenk, R. Novel ligands for a purine riboswitch discovered by RNA-ligand docking. *Chem. Biol.* **2011**, *18* (3), 324−35.
(27) Link, K. H.; Breaker, R. R. Engineering ligand-responsive gene-control elements: lessons learned from natural riboswitches. *Gene Ther.* **2009**, *16* (10), 1189−201.
(28) Penchovsky, R. Engineering gene control circuits with allosteric ribozymes in human cells as a medicine of the future. *Quality Assurance in Healthcare Service Delivery, Nursing and Personalized Medicine: Technologies and Processes*; IGI Global: Hershey, PA, 2012; p 21